Analysis of Reverse Stress in Potential Induced Degradation Affected PV Module Under Partial Shading Conditions

Asokan S[1], Vishal E. Puranik[1], Ravi Kumar[1], and Rajesh Gupta[1]

[1]Department of Energy Science and Engineering

Indian Institute of Technology Bombay, Mumbai (India)

Abstract

Potential induced degradation (PID) is a detrimental failure mechanism that has gained greater attention in medium and large-scale photovoltaic (PV) plants in a recent decade. PID reduces shunt resistance and increases the recombination diode's reverse saturation current. As a direct consequence, the efficiency of PID affected module experiences a substantial decline, often leading to module failure well before their expected operational lifespan. Further, when a PID affected cell of a module is partially or entirely shaded, reverse stress is observed across the shaded PID cell, which ultimately affects the module's reliability. This paper presents an analysis of the reverse stress across the shaded cell encountered in PID affected PV module under partial shading conditions. The findings suggest that the high reverse current flows through the PID affected cell under partial shading conditions as compared to partially shaded healthy cell. The reverse stress current across the shaded cell depends on the value of its shunt resistance. By understanding the impact of reverse stress on PID affected modules, further degradation of PV modules can be prevented, improving the performance and overall efficiency of the PV system.

Keywords: Potential induced degradation (PID), Partial shading, Reverse stress, Reliability

1. Introduction

The crystalline silicon (c-Si) solar cell is one of the widespread photovoltaic (PV) technology used worldwide for commercial applications. PV modules are supposed to work in the field for at least 25-30 years. Therefore, ensuring the reliability of photovoltaic systems is a concern for the PV community. However, in the field, PV modules are exposed to a wide range of environmental conditions that can lead to different defects and degradation, which affects the performance and reliability of PV modules (Sharma and Chandel, 2013). Common field defects and degradations reported in PV modules include corrosion, delamination, discoloration, breakages, cracks, hot spots, light induced degradation (LID), light and elevated temperature induced degradation (LeTID) and potential induced degradation (PID) (Roy, Kumar and Gupta, 2019)(Luo *et al.*, 2017). PID is a severe degradation mechanism, observed in medium and large PV system due to high system voltages. It significantly increases module degradation rates and losses in a PV system, making it one of the most critical issues in medium and large-scale PV plants. It can advance rapidly in a PV module during its initial years after installation, with a degradation rate that can be as high as 4% per year (Puranik and Gupta, 2022). PID reduces the shunt resistance (R_{sh}) and increases the reverse saturation current of the recombination diode (Kumar, Puranik and Gupta, 2023). Low shunt resistance significantly impact performance and reliability of PV module, especially under low irradiance or partial shading conditions (Barbato *et al.*, 2014, Braisaz and Radouane, 2014).

Under partial shading condition, reverse current flows through the shunt resistance of the reverse stressed shaded cell. The amount of reverse current depends on the value of the R_{sh}, amount of shading on the cell and the string current in the module (Arekar, Puranik and Gupta, 2021). Partial shading can occur due to surrounding poles, bird droppings, leaves, dirt, building towers, and trees. PV system is highly susceptible to partial shading (Teo *et al.*, 2018). A distinct correlation between the shunt resistance and the slope of the shaded cell's reverse I-V curve has been proposed in the literature (Meyer and Van Dyk, 2005). A bypass diode is used in PV module across a string to prevent highly degraded reverse stress condition i.e., hotspot. Even in the presence of bypass diode, a hotspot condition can occur if the shunt resistance of the shaded cell is sufficiently low. Under such circumstances, the PV cell may attain a temperature that can cause permanent

10.18086/swc.2023.01.01 Available at http://proceedings.ises.org

damage due to hotspot heating. This severely affect the reliability of the module (Rossi *et al.*, 2015). Therefore, it is crucial to investigate PID affected module under partial shading conditions.

This paper aims to investigate the reverse stress conditions across a PID affected cell with different extent of PID under partial shading conditions. In PSpice simulations, reverse stress current, voltage, and power dissipation are calculated at different levels of PID by adjusting the shunt resistance and photogenerated current. Same has been validated using experimentations.

The article is organized as follow: section 2 presents the approach used in this investigation, section 3 presents and discusses the results obtained and finally section 4 concludes the article.

2. Approach

Experimentation, modelling, and simulation were performed to investigate the reverse stress experienced by the PID module under shading. The solar module (Make: Sun solar, 7.5W, mc-Si based on Al- BSF technology) was used for the PID test. Initially, in order to observe existing defects, the module was characterized before the PID generation by using IV characterization and electroluminescence (EL) imaging.

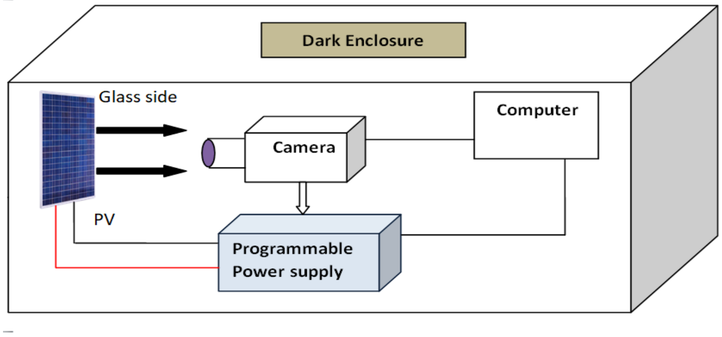

Fig. 1: Electroluminescence (EL) imaging Setup

A solar simulator has been used for the IV analysis part (make: Autosys, Model: SMT-INV 2011SF Class: BAA). The measurements were performed in accordance with standard test conditions (STC) of AM 1.5G, 1000 W/m^2 and 25 °C. It provides the performance parameters i.e., maximum output power (P_{max}), short circuit current (I_{sc}), and open circuit voltage (V_{oc}). Subsequently, for the purpose of localizing and conducting a spatial analysis of cells within PV modules, EL imaging was performed. The EL imaging setup is shown in Fig. 1. In the imaging setup, an EL camera (Make: Greateyes Gmbh) has been used. The system is equipped with a silicon-based charge-coupled device (Si-CCD) having a resolution of 1024×1024 pixels, which proves adequate for the spatial analysis required for the PID test in this study. The camera has been connected to an externally programmed power supply (TDK-Lambda, GEN150–10) for biasing the modules. The EL operation is controlled by a monitoring PC. The entire setup is enclosed within a dark chamber to minimize the impact of stray light, and the chamber's temperature is maintained at a constant 25 °C to ensure consistent measurement conditions. In the absence of light, the PV cell undergoes electrical excitation, with the EL current being less than or equal to the short-circuit current (I_{sc}). As a consequence, the cell emits an EL signal due to band-to-band radiative recombination occurring within the bulk region (Roy and Gupta, 2019).

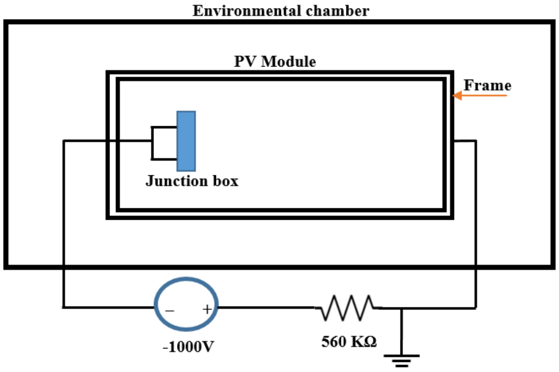

Fig. 2: Schematic diagram of PID test setup

Following the initial phases of IV characterization and EL imaging, an accelerated PID test was conducted in a controlled environmental chamber (Manufactured by REMI Instruments). Under PID testing the modules was subjected PID accelerated testing conditions (-1000 V, 60°C, 85% RH) lasting for 96 hours. PID test setup is shown in Fig. 2. EL images and IV characteristics of the PV module pre and post PID testing are shown in Fig. 3 (a), (b) and (c). Moreover, for a holistic view of the module's performance, a detailed comparison of its parameters before and after the PID test is provided in Tab 1.

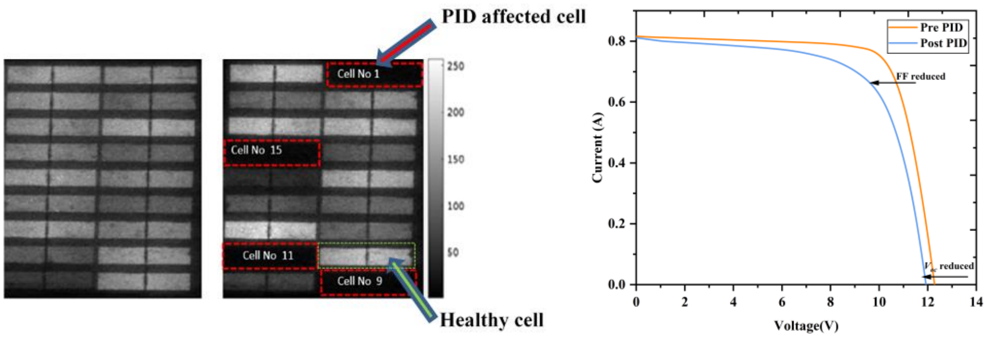

(a) **(b)** **(c)**

Fig. 3: EL images of the module (a) pre PID (b) post PID (c) pre and post PID I-V characteristics of the module

Tab.1. Module specifications pre PID and post PID

Status	**(V_{oc})**	**(I_{sc})**	**(P_m)**	**(V_m)**	**(I_m)**	**FF**
pre PID	12.27	0.81	7.54	10.05	0.75	0.76
post PID	11.9	0.81	6.35	9.49	0.67	0.66

From Tab. 1, it can be observed that PID results in a reduction in the fill factor (FF) and open circuit voltage (V_{oc}) of the PV module. The IV characteristics of solar cells, when measured under both dark and illuminated conditions, serve as a crucial tool for evaluating their performance. Therefore, destructive analysis was conducted to perform dark I-V characterization, which enable the extraction of seven parameters of the double diode model (DDM) for each cell. The DDM of a PV cell is generally used for either higher accuracy or modelling shunt-related defects such as PID (Ishaque, Salam and Taheri, 2011), as shown in Fig .3. In this context, the variables are defined as follows: I_{ph} represents the light-generated current, while I_{01}, I_{02}, n_1, and n_2 represent the saturation current and ideality factors of the bulk diode (D_1) and recombination diode (D_2), respectively. R_s and R_{sh} denote the series and shunt resistance of a PV cell.

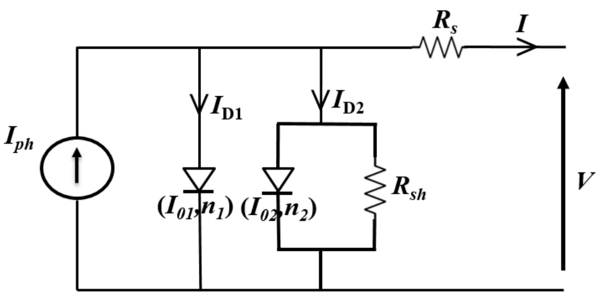

Fig. 4: Double diode model of a PV cell

$$I = I_{ph} - I_{01}\left[\exp\left(\frac{V+IR_S}{n_1 V_t} - 1\right)\right] - I_{02}\left[\exp\left(\frac{V+IR_S}{n_2 V_t} - 1\right)\right] - \frac{V+IR_S}{R_S} \quad \text{(eq. 1)}$$

Equation 1 shows the current-voltage relation of a PV cell, which contains seven unknown parameters (I_{ph}, I_{01}, I_{02}, n_1, n_2, R_s, R_{sh},), whereas V_t represents the diode thermal voltage. Double diode model simulations have been performed using PSpice, as it is a versatile tool to simulate the electrical and thermal aspects of PV modules (Somasundaran, Sinha and Gupta, 2012). Individual cell power output is determined by PSpice simulations by using parameters extracted using DDM. To confirm cells affected by PID, EL images (Post

PID) are compared with the individual cell power levels. PID-affected cells are identified by their reduced power output, evident from their darker appearance in EL images compared to healthy cells. Using the extracted parameters, impact of shading on both PID-affected and healthy cells are simulated to calculate reverse saturation current, reverse saturation voltage, and power dissipation.

3. Result and Analysis

The power loss of each cell in a PV module is depicted in Fig. 5. It is evident that the PID affect the power output. It is expected that healthy cells or those minimally impacted by PID would exhibit negligible power loss. From Fig. 5, cell no. 12 and cell no. 8 are found to be minimally PID-affected while cell no. 15 and cell no. 11 are found to be highly PID affected cells, showing more significant power losses.

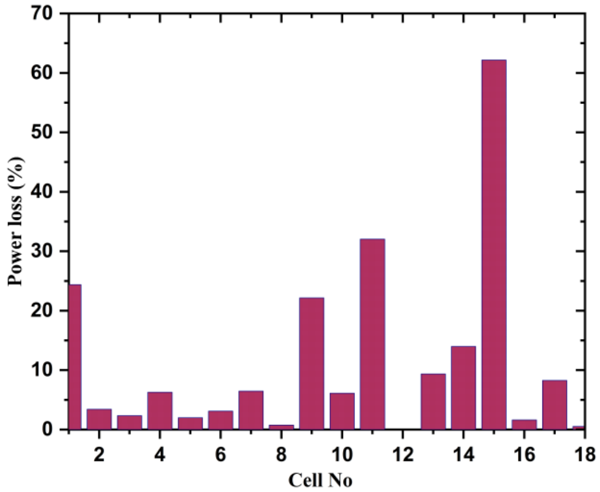

Fig. 5: Cell wise power loss of PID tested PV module

Using the above identified cells, simulations and experiment are carreid out to obtain the reverse stress current, voltage and power dissipation under partial shading condition across the healthy and PID affected.

3.1 Simulation

To analyze the reverse stress across the PID-affected cells, simulations have been performed by changing the R_{sh} and light generated current. Fig. 6(a) illustrates the reverse current, reverse voltage, and power dissipation characteristics of a healthy cell (cell no.12) under varying shading conditions, including complete shading (0 W/m²) and partial shading (200 W/m² and 500 W/m²). For the purpose of comparison, normalised reverse current (Reverse current of R_{sh} of the shaded cell / Current of R_{sh} of healthy cell without shading (nominal value)), normalised reverse voltage (Reverse voltage across R_{sh} of the shaded cell / Voltage across R_{sh} of healthy cell without shading (nominal value)), normalised power dissipation (Power dissipation of R_{sh} of the shaded cell / Power dissipation of R_{sh} of healthy cell without shading (nominal value)) have been considered.

From Fig. 6(a), it is observed that when the healthy cell is completely shaded, the reverse current through the R_{sh} is approximately eight times the nominal value. However, as the cell experiences partial shading (200 W/m² and 500 W/m²), the reverse current begins to decrease. This phenomenon can be attributed to the fact that the healthy cell possesses a substantial resistance. When shaded, the current generated by neighbouring cells starts flowing through the shaded cell, resulting in the observed reverse current in R_{sh}. Although the magnitude of current flowing through the R_{sh} is relatively low, the product of resistance and current leads to significantly elevated power dissipation levels under complete shading conditions. Remarkably, the power dissipation of the shaded cell reaches many times the nominal value when completely shaded. However, as the cell starts receiving irradiance, the reverse current diminishes, subsequently reducing both the normalized voltage and normalized power dissipation. Notably, at 500 W/m², the reverse current, reverse voltage, and power dissipation in the R_{sh} become negligible. To gain further insights, the shading effects on a slightly PID affected cell are investigated. Fig. 6(b) illustrates the shading impact on the reversse stress parameters for the slighlty affected PID cell. Notably, as PID conditions become more severe, the reverse current through the R_{sh} increases.

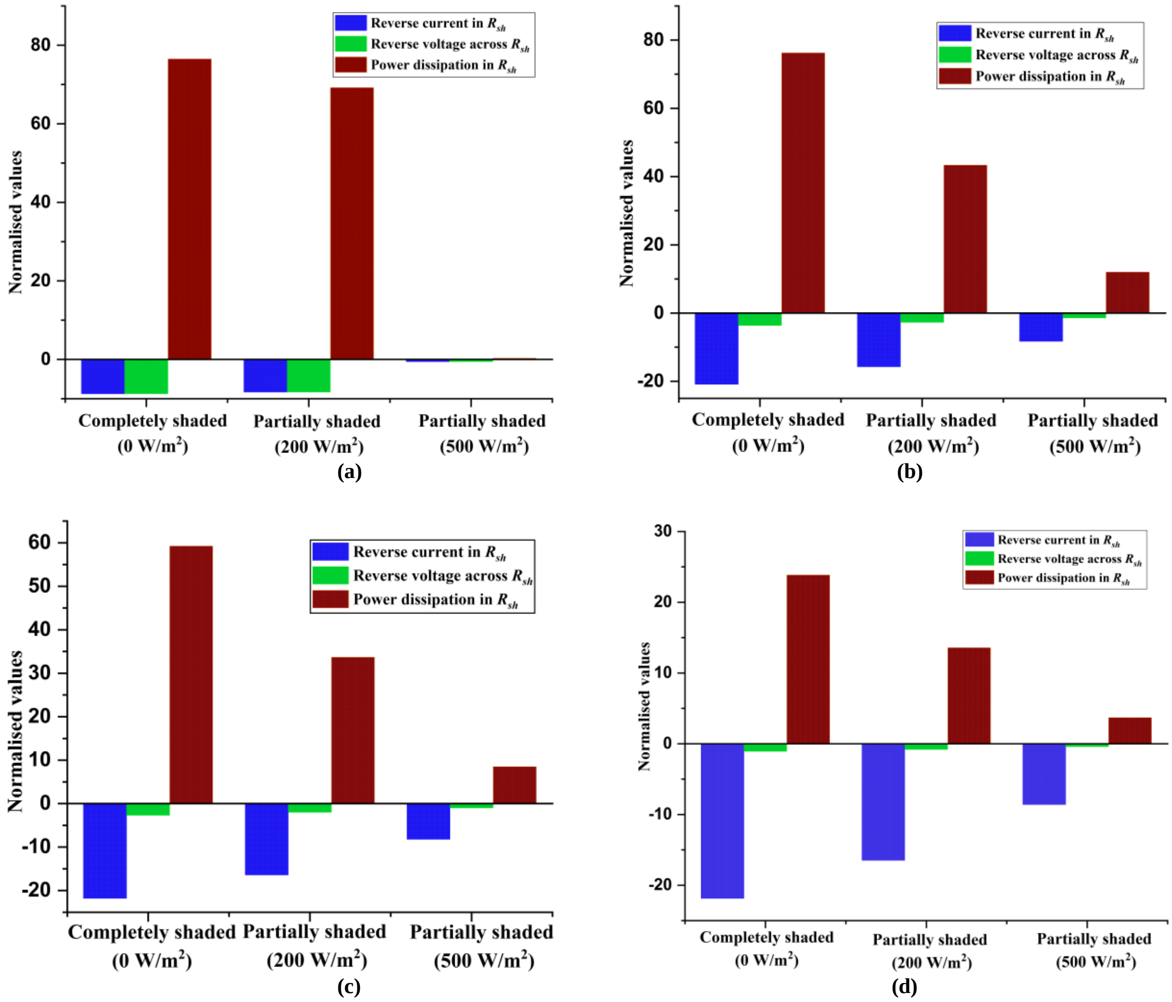

Fig. 6. Variation in reverse current, reverse voltage and power dissipation for (a) Shading on healthy cell, (b) Shading on slightly PID affected cell, (c) Shading on moderately affected PID cell, and (d) Shading on severely affected PID cell.

This phenomenon is attributed to the PID reduction in R_{sh}, causing an elevated current flow through it. Remarkably, the observed current through the R_{sh} is approximately 20 times the nominal value, a significantly higher magnitude compared to shading on a healthy cell. Conversely, the voltage across the R_{sh} experiences a reduction. This decline can be explained by the diminished product of current and resistance. Despite the decrease in voltage, the power dissipation across the shaded cell remains high, comparable to that of a healthy cell. This is because power dissipation is proportional to the square of the current multiplied by the resistance. Furthermore, as shading conditions are reduced, the reverse stresses on the cell also diminish, mirroring the trends observed in shading effects on healthy cells.

To investigate deeper into the effects of shading, a simulation on a moderately PID-affected cell was conducted. Fig. 6(c) provides a visual representation of shading versus normalized values for this moderately PID-affected cell. The observed current through the R_{sh} is approximately 21 times the nominal value, which is notably higher compared to shading on a slightly PID-affected cell. The voltage across the R_{sh} undergoes a reduction due to the decreasing value of R_{sh}. Moreover, as shading conditions decrease, the reverse stresses also decrease, like the trends observed in shading on slightly PID-affected cells. It is evident that the power dissipation in the moderately PID-affected cell is approximately 60 times the nominal value, which is significantly high.

Fig. 6(d) shows the shading effects on a cell severely impacted by PID, which highlights the extreme nature of the PID severity. This very severely PID-affected cell has experienced a complete loss of power due to the extreme severity of PID, resulting in a significant reduction in the R_{sh} value. As a result, there is a substantial surge in the reverse current flowing through the R_{sh}. Notably, Fig. 6(d) demonstrates that the current through the R_{sh} reaches approximately 23 times the nominal value. Simultaneously, the voltage across both the R_{sh} and the cell itself experiences a profound reduction, primarily attributed to the substantial decrease in shunt resistance. As the PID severity intensifies, so does the impact on the cell's electrical characteristics, leading to increasingly adverse effects. It is crucial to highlight that as shading conditions are diminished, the reverse stresses on the cell diminish accordingly; it agrees with the trends observed in shading on severely PID-affected cells. Remarkably, the power dissipation in the severely PID-affected cell decreases to approximately 20 times the nominal value. While this figure remains notably elevated, it represents a significant reduction compared to shading on severely affected PID cells. However, it's essential to emphasize that the high reverse current flowing through R_{sh} can have detrimental consequences for the cell's reliability. When a low R_{sh} cell is shaded, the concentration of high reverse current in a localized area raises the risk of hotspot formation. This underscores the critical importance of addressing and mitigating severe PID effects to preserve the overall reliability and performance of photovoltaic systems.

3.2 Experimental validation:

To validate the simulation results, experimentation has been performed on a PID-affected module. The identified PID cells are shaded by using cardboard, and each cell is accessed through destructive analysis. CRO (Make: Yogowa, Model: DL850E) is connected across each cell, and I-V characterization has been performed.

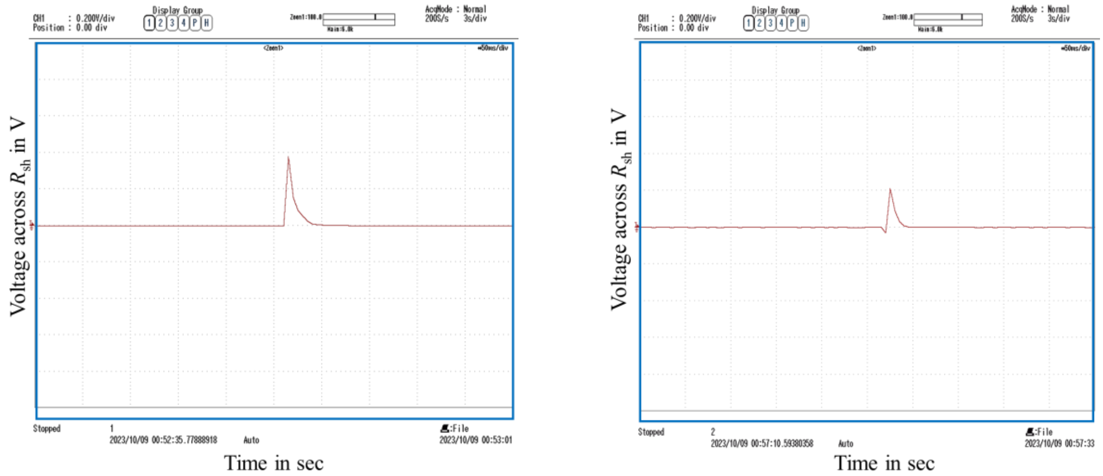

(a) **(b)**

Fig. 7: Voltage across R_{sh} without shading for (a) healthy cell and (b) PID-affected cell

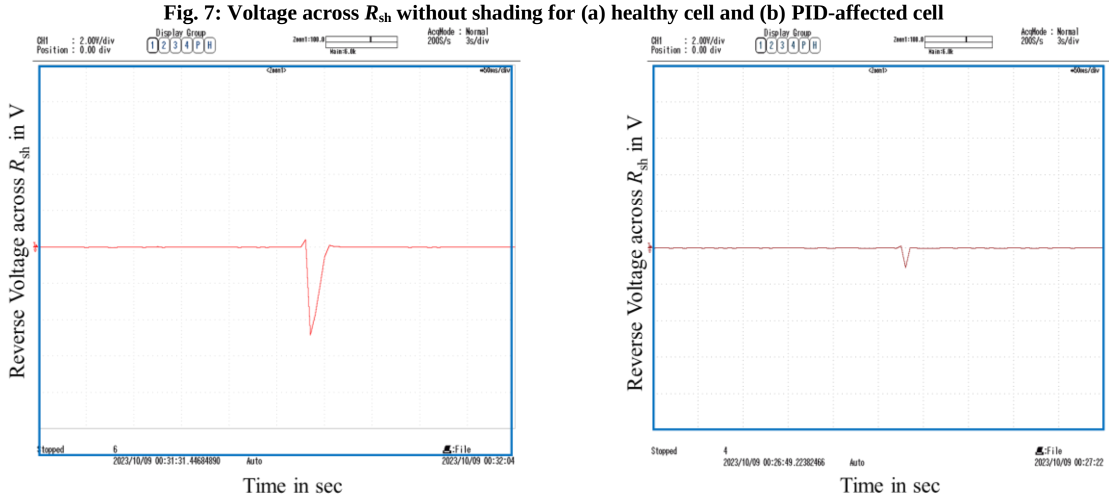

(a) **(b)**

Fig. 8: Reverse voltage across R_{sh} with shading for (a) healthy cell and (b) PID-affected cell

In Fig. 7(a), the voltage across the healthy cell in an unshaded condition is depicted. It is evident that the shunt resistance sinks the current, resulting in a positive voltage across the cell. Similarly, in Fig. 7(b), the voltage across the PID-affected cell without shading is illustrated. Notably, the voltage across the PID-affected cell is lower than that of the healthy cell due to the reduced R_{sh}.

The findings showcased in Fig. 8(a) offer a significant insight into the performance of a healthy cell under shading conditions. From this, the reverse voltage characteristics of a healthy cell when it is fully shaded are observed. Notably, it reveals that the reverse voltage across the healthy cell substantially rises when subjected to shading. This observation serves as a remarkable agreement between the experimental results and the simulated outcomes.

Fig. 8(b) represents the reverse voltage across a severely PID-affected cell when shaded. It can be noted that the reduction in voltage across the R_{sh} for PID affected cell is lower than that of the healthy cell for shaded conditions. This observed reduction in voltage corresponds well with the results obtained from simulation.

4. Conclusion

In this work, impact of PID on reverse stress current, voltage and power dissipation across the partial shaded cell in a PV module is investigated. Reverse stress parameters i.e., current, voltage and power dissipation are calculated for healthy and PID affected PV cells in a PV module using PSpice simulations. The reverse current across the shaded cell increases with PID progression which maximises under completely shaded condition while the reverse voltage and power dissipation across the shaded cell decreases. Reverse voltage trend with PID progression obtained experimentally successfully support the simulation results. A high current across the PID affected cell poses a risk of hotspot formation. The value of the reverse current, voltage and power dissipation across the shaded cell depends on the PID severity and amount of shading. The obtained results provide a valuable insights into the behaviour of PID affected PV cells under partial shading conditions.

5. References

Arekar, K., Puranik, V. E. and Gupta, R. (2021) 'Performance Analysis of PID Affected Crystalline Silicon PV Module under Partial Shading Condition', *Conference Record of the IEEE Photovoltaic Specialists Conference*, pp. 2415–2420. doi: 10.1109/PVSC43889.2021.9518533.

Barbato, M. *et al.* (2014) 'Influence of shunt resistance on the performance of an illuminated string of solar cells: Theory, simulation, and experimental analysis', *IEEE Transactions on Device and Materials Reliability*, 14(4), pp. 942–950. doi: 10.1109/TDMR.2014.2347138.

Braisaz, B. and Radouane, K. (2014) 'PID results at low irradiances on c-Si modules', *2014 IEEE 40th Photovoltaic Specialist Conference, PVSC 2014*, pp. 1993–1996. doi: 10.1109/PVSC.2014.6925316.

Guechi, A., Chegaar, M. and Aillerie, M. (2012) 'Environmental effects on the performance of nanocrystalline silicon solar cells', *Energy Procedia*, 18(1), pp. 1611–1623. doi: 10.1016/j.egypro.2012.06.001.

Ishaque, K. *et al.* (2011) 'Modeling and simulation of photovoltaic (PV) system during partial shading based on a two-diode model', *Simulation Modelling Practice and Theory*, 19(7), pp. 1613–1626. doi: 10.1016/j.simpat.2011.04.005.

Ishaque, K., Salam, Z. and Taheri, H. (2011) 'Simple, fast and accurate two-diode model for photovoltaic modules', *Solar Energy Materials and Solar Cells*, 95(2), pp. 586–594. doi: 10.1016/j.solmat.2010.09.023.

Kumar, R., Puranik, V. E. and Gupta, R. (2023) 'Application of Infrared Thermography for Cell-Level Power Estimation of PID-s Impacted Crystalline Silicon PV Module', *IEEE Journal of Photovoltaics*, 13(1), pp. 141–149. doi: 10.1109/JPHOTOV.2022.3229485.

Luo, W. *et al.* (2017) 'Potential-induced degradation in photovoltaic modules: A critical review', *Energy and Environmental Science*, 10(1), pp. 43–68. doi: 10.1039/c6ee02271e.

Meyer, E. L. and Van Dyk, E. E. (2005) 'The effect of reduced shunt resistance and shading on photovoltaic module performance', *Conference Record of the IEEE Photovoltaic Specialists Conference*, pp. 1331–1334. doi: 10.1109/pvsc.2005.1488387.

Puranik, V. E. and Gupta, R. (2021) 'Novel Quantitative Electroluminescence Method for Detailed Performance Analysis of PID-s Affected Crystalline Silicon PV Module', *IEEE Journal of Photovoltaics*, 11(6), pp. 1470–1478. doi: 10.1109/JPHOTOV.2021.3108764.

Puranik, V. E. and Gupta, R. (2022) 'Analysis and insight of electroluminescence imaging in the assessment of potential-induced degradation in crystalline silicon photovoltaic module', *Engineering Failure Analysis*, 134(October 2021), p. 106027. doi: 10.1016/j.engfailanal.2022.106027.

Rossi, D. *et al.* (2015) 'Modeling and detection of hotspot in shaded photovoltaic cells', *IEEE Transactions on Very Large Scale Integration (VLSI) Systems*, 23(6), pp. 1031–1039. doi: 10.1109/TVLSI.2014.2333064.

Roy, S. and Gupta, R. (2019) 'Non-destructive approach for severity investigation of shunts in crystalline silicon photovoltaic modules by combination of electroluminescence imaging and lock-in thermography', *Measurement Science and Technology*, 30(4). doi: 10.1088/1361-6501/ab0265.

Roy, S., Kumar, S. and Gupta, R. (2019) 'Investigation and analysis of finger breakages in commercial crystalline silicon photovoltaic modules under standard thermal cycling test', *Engineering Failure Analysis*, 101, pp. 309–319. doi: 10.1016/J.ENGFAILANAL.2019.03.031.

Sharma, V. and Chandel, S. S. (2013) 'Performance and degradation analysis for long term reliability of solar photovoltaic systems: A review', *Renewable and Sustainable Energy Reviews*, 27, pp. 753–767. doi: 10.1016/j.rser.2013.07.046.

Somasundaran, P., Sinha, A. and Gupta, R. (2012) 'Simulation and characterization of spatial variation of shunts in industrial solar cells by PSPICE and dark lock-in infrared thermography', *27th European Photovoltaic Solar Energy Conference and Exhibition*, (September), pp. 744–748.

Teo, J. C. *et al.* (2018) 'Impact of partial shading on the P-V characteristics and the maximum power of a photovoltaic string', *Energies*, 11(7). doi: 10.3390/en11071860.